

## Ternary MgTiX-Alloys: A Promising Route towards Low-Temperature, High-Capacity, Hydrogen-Storage Materials

Paul Vermeulen,<sup>[a]</sup> Emile F. M. J. van Thiel,<sup>[b]</sup> and Peter H. L. Notten\*<sup>[a, b]</sup>

**Abstract:** In the search for hydrogen-storage materials with a high gravimetric capacity, Mg<sub>y</sub>Ti<sub>(1-y)</sub> alloys, which exhibit excellent kinetic properties, form the basis for more advanced compounds. The plateau pressure of the Mg–Ti–H system is very low ( $\approx 10^{-6}$  bar at room temperature). A way to increase this pressure is by destabilizing the metal hydride. The foremost effect of incorporating an additional element in the binary Mg–Ti system is, therefore, to decrease the stability of the metal hydride. A model to calculate the effect on the thermodynamic stability of alloying metals was developed by Miedema and co-work-

ers. Adopting this model offers the possibility to select promising elements beforehand. Thin films consisting of Mg and Ti with Al or Si were prepared by means of e-beam deposition. The electrochemical galvanostatic intermittent titration technique was used to obtain pressure-composition isotherms for these ternary materials and these isotherms reveal a reversible hydrogen-storage capacity of more than 6 wt.%. In line with the calculations, substitu-

tion of Mg and Ti by Al or Si indeed shifts the plateau pressure of a significant part of the isotherms to higher pressures, while remaining at room temperature. It has been proven that, by controlling the chemistry of the metal alloy, the thermodynamic properties of Mg-based hydrides can be regulated over a wide range. Hence, the possibility to increase the partial hydrogen pressure, while maintaining a high gravimetric capacity creates promising opportunities in the field of hydrogen-storage materials, which are essential for the future of the hydrogen economy.

**Keywords:** dopants • hydrogen storage • metal hydrides • Miedema model • thermodynamics

### Introduction

Depleting fossil fuel reserves and growing climate threats urge us towards a sustainable society.<sup>[1]</sup> Hydrogen is expected to play a dominant role in future energy scenarios. However, the feasibility of hydrogen production, storage and final end-use are still under debate. Hydrogen is usually produced by the steam reforming of fossil fuels, by partial oxidation of natural gas and by coal gasification. These methods, however, still require fossil fuels and therefore, do not address the problems related to our declining energy

sources. An alternative method to generate hydrogen is electrolysis of water, but it is generally considered to be inefficient. Other techniques to produce hydrogen include high-temperature electrolysis, which can increase the efficiency significantly, and hydrogen generation through the chemical reactions of certain alga (e.g., *Scenedesmus*).<sup>[2,3]</sup>

In prototype applications, such as fuel-cell-driven automobiles, hydrogen is generally stored in high-pressure cylinders. New lightweight composite cylinders have been developed which are able to withstand pressures of up to 800 bars. Even though hydrogen cylinders are expected to withstand even higher pressures in the near future, their large volumes and the energy required to compress hydrogen will limit their practical applicability. As opposed to storing molecular hydrogen it can also be stored chemically in a metal hydride (MH), which can reduce the volume significantly. In addition, MHs provide relatively safe storage as they can be handled without extensive safety precautions unlike, for example, compressed hydrogen gas.

Currently, the foremost problem of solid state storage is to find a metal-hydrogen system with a gravimetric capacity that exceeds 6 wt.%H and absorbs/desorbs hydrogen at at-

[a] P. Vermeulen, Prof. Dr. P. H. L. Notten  
Department of Chemical Engineering and Chemistry  
Eindhoven University of Technology  
Den Dolech 2, 5600 MB Eindhoven (The Netherlands)  
Fax: (+31) 40-2455-054  
E-mail: P.Vermeulen@tue.nl  
Peter.Notten@philips.com

[b] E. F. M. J. van Thiel, Prof. Dr. P. H. L. Notten  
Philips Research Laboratories  
Prof. Holstlaan 4 (WAG02), 5656 AA Eindhoven (The Netherlands)  
Fax: (+31) 40-274-3352

mospheric pressures and at ambient temperatures.<sup>[4]</sup> In spite of the fact that MgH<sub>2</sub> satisfies the requirement set by the U.S. Department of Energy, with a theoretical capacity of 7.6 wt. %H, its high thermodynamic stability, resulting in a low partial hydrogen pressure ( $P_{\text{H}_2}$ ) at ambient temperatures, prevents it from being adopted as H storage material. Moreover, MgH<sub>2</sub> suffers from slow (de)hydrogenation kinetics.<sup>[5]</sup> Unfortunately, the history of enhancing the thermodynamics of MgH<sub>2</sub> to an appreciable degree is quite dismal. Among the improvements is Mg<sub>2</sub>Ni that enables 1 bar H<sub>2</sub> pressure at 255 °C, which is 24 °C lower compared to MgH<sub>2</sub>.<sup>[6–8]</sup>

Recently, promising new hydrogen-storage alloys were reported that consist of Mg and Ti.<sup>[9–12]</sup> Electrochemical measurements showed that adding Ti positively affects the kinetics of hydride formation compared to MgH<sub>2</sub>. Furthermore, the attractive storage capacity of MgH<sub>2</sub> was preserved to a large extent and the reversibility of hydrogen insertion and extraction was found to be robust. In the present paper it will be shown that the plateau pressure of Mg<sub>y</sub>Ti<sub>(1–y)</sub> alloys is of the order of 10<sup>–6</sup> bar at room temperature. The appealing kinetic properties of Mg<sub>y</sub>Ti<sub>(1–y)</sub> make this material a good starting-point for the development of more advanced, thermodynamically less stable, MHs.

A mathematical model to calculate the effect of adding an additional element in a metallic compound on the thermodynamic stability was proposed by Miedema et al.<sup>[13–15]</sup> Combined with Van Mal's rule of reversed stability,<sup>[16]</sup> it enables us to carefully select an element that is expected to enforce a destabilizing effect on the Mg–Ti–H system and, consequently, increase the partial hydrogen pressure. Al and Si were selected by adopting this approach. Several ternary compositions were prepared and their hydrogen-storage characteristics were determined electrochemically. The effects of incorporating Al and Si in the Mg–Ti lattice on the hydrogen-storage properties are discussed in this paper.

## Results and Discussion

The  $P_{\text{H}_2}$  of a MH is related to its thermodynamic stability by means of the Van't Hoff-equation [Eq. (1)].<sup>[17,18]</sup>

$$\ln P_{\text{H}_2} = \frac{\Delta H_f}{RT} - \frac{\Delta S_0}{R} \quad (1)$$

The value of  $\Delta H_f$  is the enthalpy of formation,  $R$  the universal gas constant,  $T$  the absolute temperature,  $\Delta S_0$  is the entropy of formation in JK<sup>–1</sup> molH<sub>2</sub>. In a first approximation,  $\Delta S_0$  is mainly determined by the loss of entropy when gaseous H<sub>2</sub> is absorbed in the solid, that is,  $\Delta S_0 \approx -\Delta S_{\text{H}_2} = -130.8 \text{ JK}^{-1} \text{ mol H}_2$ . Equation (1) shows that in order to increase  $P_{\text{H}_2}$ , the metal-hydrogen system can be destabilized by increasing  $\Delta H_f$ . A possible route to destabilize a MH is by increasing the stability of the metallic compound. This principle is known as the rule of reversed stability, introduced by Van Mal et al.,<sup>[16]</sup> which states that the more stable

a metallic alloy is the less stable its hydride will be. Combined with the Miedema model it enables us to select an element, which is expected to impose a destabilizing effect on the metal system, thus increasing the partial hydrogen pressure of the MH. Notably, although the composites of interest consist of three elements, the common binary approach of the Miedema model is chosen because of its simplicity. Consequently, the results are a first-order approximation and can only be dealt with qualitatively.

The Miedema model uses different equations to determine  $\Delta H_f$  for binary alloys between two non-transition metals and between a non-transition metal and a transition metal. The former is denoted as Equation (2)

$$\Delta H_f = \frac{2f(c_A V_A^{2/3} + c_B V_B^{2/3})}{(n_{\text{WS}}^A)^{-1/3} + (n_{\text{WS}}^B)^{-1/3}} \cdot (-P(\Delta\varphi^*)^2 + Q(\Delta n_{\text{WS}}^{1/3})^2) \quad (2)$$

The value of  $f$  accounts for the concentration dependence of  $\Delta H_f$  for ordered compounds,  $V_A$  and  $V_B$  are the molar volumes of the elements inside the alloy,  $n_{\text{WS}}^A$  and  $n_{\text{WS}}^B$  are the electron densities of elements A and B at the boundary of their Wigner-Seitz cell.  $\Delta\varphi^* = \varphi_A^* - \varphi_B^*$  represents the difference in electronegativity between elements A and B.  $P$  and  $Q$  are experimentally determined parameters and depend on the elements involved in the alloy.

The enthalpy of formation of an alloy consisting of a non-transition metal and a transition metal is described by Equation (3).

$$\Delta H_f = \frac{2Pf(c_A V_A^{2/3} + c_B V_B^{2/3})}{(n_{\text{WS}}^A)^{-1/3} + (n_{\text{WS}}^B)^{-1/3}} \cdot \left( -(\Delta\varphi^*)^2 + \frac{Q}{P}(\Delta n_{\text{WS}}^{1/3})^2 - \frac{R}{P} \right) \quad (3)$$

The value of  $R/P$  is the so-called hybridization term, which represents the degree of mixing of d-states of the transition metal with the s-state of the non-transition metal.

As the Mg–Ti–H system is characterized by a high gravimetric capacity, only lightweight elements are regarded as promising substitutes. These elements should preferably be cheap and readily available. On the basis of these criteria Al and Si were selected and both offer the additional advantage that their individual hydrides are relatively unstable, which is expected to impose a positive effect on the stability of the MgTiX (X = Al, Si) hydride. The values of the parameters required to calculate  $\Delta H_f$  of the binary constituents of Mg–Ti doped with Al or Si are listed in Table 1. The values

Table 1. Parameters required for the Miedema model.<sup>[14]</sup>

Element	$\varphi^*$ [V]	$n_{\text{WS}}^{1/3}$ [(d.u.) <sup>1/3</sup> ] <sup>[a]</sup>	$V^{2/3}$ [cm <sup>2</sup> ]
Mg	3.45	1.17	5.8
Ti	3.65	1.47	4.8
Al	4.20	1.39	4.6
Si	4.70	3.38	4.2

[a] d.u. = density units.

for  $P$  are 10.6 and 12.3 for binary alloys of two non-transition metals and a transition metal with a non-transition metal, respectively. For all solid state alloys  $Q/P$  equals  $9.4 V^2 (\text{d.u.})^{-2/3}$  (d.u. = density units) and  $R/P$  for Mg–Ti, Al–Ti and Si–Ti equals 0.4, 1.9 and 2.1, respectively. The results of the calculated enthalpy of formation for the various binary alloys are depicted in Figure 1.

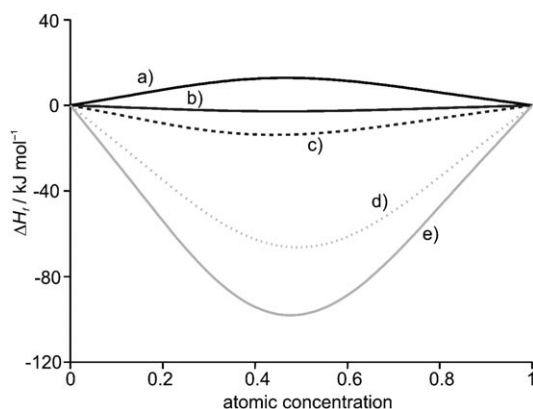


Figure 1.  $\Delta H_f$  as a function of composition for a) Mg in Ti, b) Mg in Al, c) Mg in Si, d) Ti in Al and e) Ti in Si.

Figure 1 shows that incorporating Al or Si into the Mg–Ti system (a) both stabilize the ternary alloy as Mg–Al (b), Mg–Si (c) and to an even larger extent Ti–Al (d) and Ti–Si (e) are characterized by a relatively low enthalpy of formation. The positive values of  $\Delta H_f$  for the Mg–Ti system are in line with the literature as no intermetallics are reported for this particular alloy if standard alloying techniques are used.<sup>[19]</sup> However, using electron beam deposition, direct current/radio frequency magnetron co-sputtering and mechanical alloying it is possible to obtain homogenous Mg–Ti alloys that are regarded metastable.<sup>[9–12,20]</sup>

To verify if the partial hydrogen pressure indeed changes by incorporating Al and Si in the Mg–Ti crystal lattice, pressure-composition (PC) isotherms of these alloys are measured electrochemically by means of the galvanostatic intermittent titration technique (GITT). This method is explained below.

Generally, (de)hydrogenation of a metal (M) is often conducted using hydrogen gas. However, because the absolute amount of hydrogen stored in a thin metal film is very small, it is virtually impossible to determine the hydrogen content from gas phase experiments. Therefore, inserting and extracting hydrogen electrochemically is considered an indispensable technique to investigate new hydrogen-storage materials, as it allows an accurate determination of the hydrogen concentration in a thin film.

Electrochemical (de)hydrogenation of a metal in an alkaline electrolyte occurs by means of Equation (4).<sup>[21]</sup>



Subsequently, the adsorbed hydrogen atoms ( $\text{H}_{\text{ad}}$ ) is absorbed by the metal ( $\text{H}_{\text{abs}}$ ), represented by Equation (5).



Under hydrogenation conditions a parasitic reaction, known as the hydrogen evolution reaction (HER), can occur according to Equation (6).



One of the most important properties of a metal-hydrogen system to be used in future applications is the hydrogen plateau pressure, the pressure at which the hydrogen-poor  $\alpha$ -phase transforms to the  $\beta$ -phase as a function of hydrogen content and vice versa. The partial hydrogen pressure ( $P_{\text{H}_2}$ ) of a metal hydride is related to the equilibrium potential ( $E^{\text{eq}}$ ) represented in Equation (7).<sup>[21,22]</sup>

$$E^{\text{eq}} = -\frac{RT}{2F} \ln \frac{P_{\text{H}_2}}{P_{\text{ref}}} \text{ vs. RHE} \quad (7)$$

The value of  $F$  is the Faraday constant,  $P_{\text{ref}}$  is the reference pressure (1 bar) and RHE refers to the reversible hydrogen electrode. In the present experiments, the more practical Hg/HgO reference electrode, immersed in a 6M KOH solution, is used. Consequently, a constant to account for this reference electrode has to be added to Equation (7), according to Equation (8).

$$E^{\text{eq}} = -\frac{RT}{2F} \ln \frac{P_{\text{H}_2}}{P_{\text{ref}}} - 0.931 \quad (8)$$

To obtain values for  $E^{\text{eq}}$  at different hydrogen contents GITT is used. This method is based on collecting equilibrium potential data by applying a current pulse, followed by a current-off relaxation period. A single current step and resulting electrochemical potential response are schematically illustrated in Figure 2.

Starting at an equilibrium state, characterized by  $E_1^{\text{eq}}$  the potential of the metal hydride ( $E$ ) changes when the current

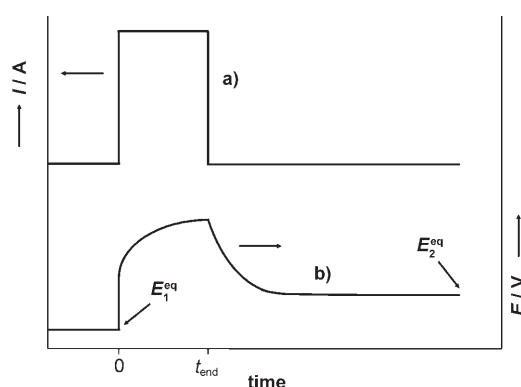


Figure 2. a) Current pulse applied to the metal hydride electrode and b) the resulting potential response. The equilibrium potentials before ( $E_1^{\text{eq}}$ ) and after ( $E_2^{\text{eq}}$ ) the current pulse are indicated.

is switched on at  $t=0$ . At  $t=t_{end}$  the current is interrupted and  $E$  relaxes toward a new equilibrium state ( $E_2^{eq}$ ). The difference between  $E_1^{eq}$  and  $E_2^{eq}$  is a result of the difference in hydrogen content, which can be exactly calculated from the amount of charge ( $Q$ ) that is inserted or extracted during the current pulse.  $Q$  can be quantified by integrating the current with respect to time ( $t$ ), according to Equation (9)

$$Q = \int_0^{t_{end}} I dt \quad (9)$$

Using the Faraday constant,  $Q$  can easily be converted to the amount of absorbed moles of H, as every electron corresponds to a single H atom that is inserted or extracted [see Eq. (4)] by means of Equation (10).

$$\frac{Q}{F} = \text{mole H} \quad (10)$$

Several current steps and relaxation periods are applied to obtain values of  $E^{eq}$  that are related to partial hydrogen pressures by using Equation (8). By plotting these values as a function of H-content yields, the required pressure-composition isotherms can be acquired.

Electrochemically obtained isothermal curves are generally determined under dehydrogenation conditions as incorrect calculations of the H-content caused by the parasitic HER [Eq. (6)] are then avoided. Since conventional gas-phase pressure-composition-temperature (PCT) measurements are generally represented with increasing hydrogen content, the electrochemically determined isotherms in the present paper are also plotted in accordance with this convention. The pressure-composition characteristics of the  $Mg_yTi_zX_{(1-y-z)}$  alloys ( $X=Al, Si$ ), alloys are determined using current pulses of  $12 \mu A$  ( $\approx 100 \text{ mA g}^{-1}$ ) for a period corresponding to approximately 20 pulses to fully dehydrogenate the metal hydrides. The relaxation period after a current pulse is 1 hour. As soon as the cut-off voltage of 0 V is reached, the GITT experiment is terminated to avoid oxidation of the electrode material.

The isotherms of  $Mg_{0.69}Ti_{0.21}Al_{0.10}$  and  $Mg_{0.80}Ti_{0.20}$  thin films are depicted in Figure 3. The latter is representative for  $Mg_yTi_{(1-y)}$  alloys within the range  $0.70 \leq y \leq 0.85$  as they all reveal a single low pressure plateau. The isothermal curve of the  $Mg_{0.69}Ti_{0.21}Al_{0.10}$  compound, on the other hand, shows two plateau-like regions, a plateau up to 4 wt.% H at  $\approx 10^{-6}$  bar and a second sloping plateau at higher pressures. Apparently, incorporating Al in the Mg–Ti lattice creates interstitial sites, which can be occupied by hydrogen with a relatively positive enthalpy of formation. The occurrence of a second plateau suggests a second phase-transformation. The in situ XRD measurements are currently being performed to unambiguously clarify the crystallographic properties. Metal–hydrogen systems with two plateaus are not uncommon and were identified for the hydrides of  $Mg_2CuAl_{0.375}$ ,  $LaCo_6$ ,  $TiFe$  and  $NdCo_5$ .<sup>[23–26]</sup> However, for the

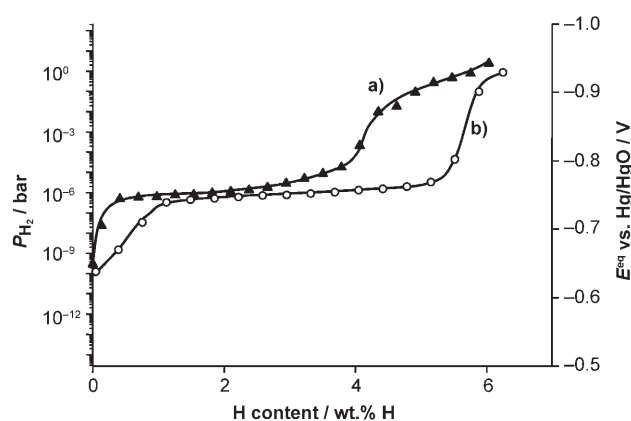


Figure 3. Electrochemically determined dehydrogenation isotherms of 200 nm; a)  $Mg_{0.69}Ti_{0.21}Al_{0.10}$  and b) and  $Mg_{0.80}Ti_{0.20}$  thin films with a 10 nm Pd top-coat.

Mg/Ti/Al/H system the isotherm interestingly shows a plateau close to atmospheric pressures at room temperature! Hence, it could be used to store and release hydrogen at low temperatures, which is of prime importance for most hydrogen-driven devices. Notably, the experimental set-up, limits the practical accessible partial hydrogen pressure to a maximum of 1 bar. Therefore, it is possible that the reversible hydrogen-storage capacity is even larger than the indicated 6 wt.% H.

Adding Al to a metal–hydrogen system to increase  $P_{H_2}$  of  $MgH_2$  has been reported by others.<sup>[27–33]</sup> However, for Mg–Al alloys it is generally observed that upon hydrogenation, the alloys disproportionate under the formation of  $MgH_2$  and Al. The PC isotherms of  $Mg_{0.69}Ti_{0.21}Al_{0.10}$  and  $Mg_{0.80}Ti_{0.20}$  depicted in Figure 3 show an almost similar reversible H-capacity of approximately 6 wt.% H, which suggests that Al actively participates in the hydrogenation process and, thus, contributes to the overall hydrogen-storage capacity.

Note that the H-content in Figure 3 corresponds to the amount that could be dehydrogenated at room temperature. These are not the absolute amounts of hydrogen in the crystal lattice of the alloy, as electrochemical measurements have indicated that part of the hydrogen is irreversibly bound. This observation is in accordance with our recent results of electrochemical (de)hydrogenation of  $Mg_yTi_{(1-y)}$  alloys with  $0.50 \leq y \leq 1.00$ .<sup>[9–11]</sup> The reversibility of hydrogen insertion and extraction, amounts to approximately 10 cycles for the electrochemical experiments, which is similar as the Mg–Ti alloys. Hereafter, delamination is considered to be the cause of the declining capacity. Therefore it is to be expected that the intrinsic reversibility of Mg–Ti–Al compounds, easily surpasses 100 cycles, as was found for the gas-phase (de)hydrogenation of Mg–Ti alloys.<sup>[34]</sup>

The H-storage capacities for the proposed ternary systems are studied in more detail as a function of composition. Figure 4 and Figure 5 show the results in combination with 3D fits obtained using a triangle-based linear interpolation Matlab® procedure (griddata). The graphs in Figures 4 and 5 are scaled to embed only the experimental range.

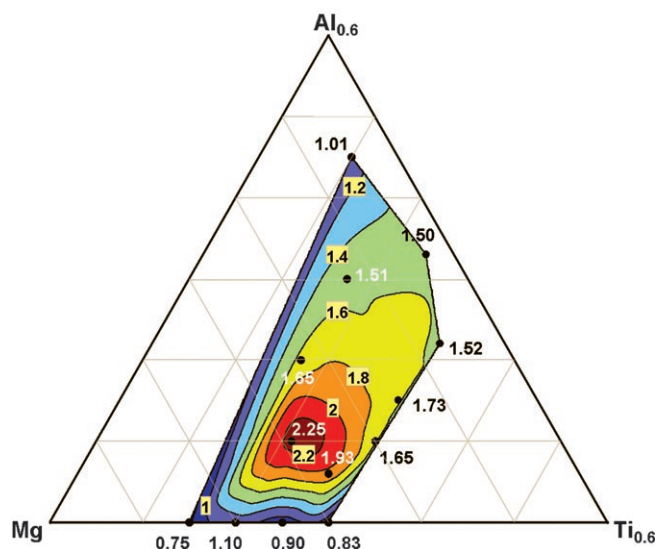


Figure 4. Phase diagram showing the compositions measured experimentally (●) in combination with the width of the isotherm situated above the first plateau in wt.%H. The values in the framed yellow labels correspond to the calculated contour lines.

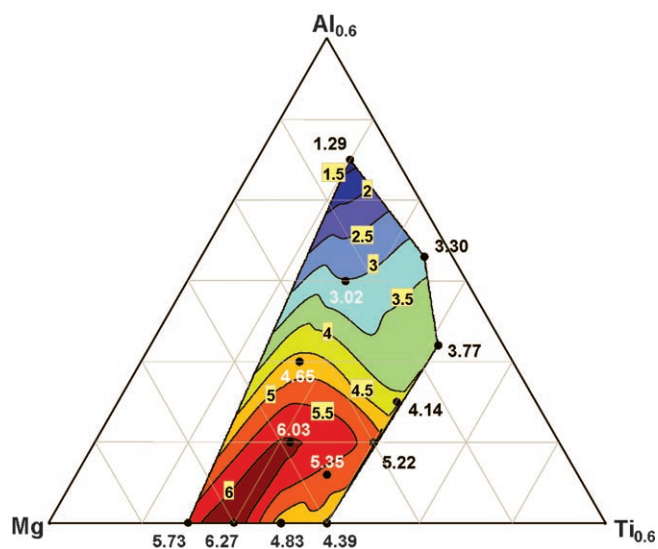


Figure 5. Phase diagram showing the reversible gravimetric H-storage capacity as a function of composition (●) with the values representing the gravimetric capacity given in wt.%H. The values corresponding to the contour lines are depicted in the framed yellow labels.

Figure 4 shows the width of isotherm that is situated above the partial hydrogen pressure of the first plateau as a function of composition and allows the reader to see that even within a small composition range the width differs significantly. All experimental data points are indicated together with the contour lines obtained from the 3D-fit. It indeed shows that adding Al to a Mg–Ti alloy changes the position of the isothermal curve to a large extent. The composition characterized by the broadest plateau situated close to at-

mospheric pressures is  $\text{Mg}_{0.69}\text{Ti}_{0.21}\text{Al}_{0.10}$ . This composition is positioned within the dark red area of Figure 4 and, according to the fit, similar or potentially even broader plateaus are to be expected in this area.

Figure 5 depicts the reversible gravimetric capacity of  $\text{Mg}_y\text{Ti}_z\text{Al}_{(1-y-z)}$  as a function of composition. It shows that incorporating Al in the Mg–Ti lattice leads to a decrease of the reversible capacity. Similar results were found for Mg–Ti–Al systems reported by Lupu et al.<sup>[35]</sup> However, the compounds they investigated have a rather high Al content and, as Figure 5 clearly indicates, this leads to a low reversible hydrogen capacity as opposed to the Mg-rich alloys presented here. If only 10 wt.% Al is incorporated into Mg–Ti compounds with a high Mg content does not seem to significantly affect the reversible capacity. The declining capacity at high Al contents could be a result of kinetic restrictions imposed by the material. These restrictions might be related to an unfavourable crystal structure of the metal hydride. Previous studies of Mg–Ti–H systems imply that the kinetics of the hydrogen insertion and extraction are largely dominated by the Mg-content. In more detail, if the metal hydride crystallizes into the rutile-like  $\text{MgH}_2$  structure the H-transportation properties are dramatically inhibited, while the kinetics is very favourable for fluorite-structured  $\text{Mg}_y\text{Ti}_{(1-y)}\text{H}_x$  alloys.<sup>[9–12]</sup> Ongoing in-situ XRD measurements are currently underway to clarify the effects of Al on the crystal lattice of Mg/Ti/Al/H.

From Figures 4 and 5 it can be concluded; that only within a small region, possible improvements of the reversible H-content at low temperatures are expected. It is, therefore, noteworthy that significant enhancements are foreseen only by incorporating a fourth element.

In the previous section it was shown that Al, in line with calculations based on the Miedema model, can advantageously affect the position of the isothermal curve in comparison to Mg–Ti alloys. The Miedema model shows that not only Al but also Si could bring about these improvements (see Figure 1). Two Si-containing Mg–Ti compounds were experimentally investigated to verify if indeed the isotherm is influenced. The results are shown in Figure 6. Note that these results are preliminary results without searching for the most optimal composition.

After an evaluation of Figure 6 it is apparent that incorporating Si clearly affects the position of the isotherms compared to Mg–Ti alloys (see Figure 3). For the Mg–Ti–Si alloys a similar shape is found, as is observed for MgTiAl (Figure 3). The value of  $P_{\text{H}_2}$  increases steeply at approximately 2.75 wt.%H and soon reaches a sloping plateau. This plateau is, similar to Al-addition, situated close to atmospheric pressures. The gravimetric reversible storage capacities of  $\text{Mg}_{0.55}\text{Ti}_{0.35}\text{Si}_{0.10}$  and  $\text{Mg}_{0.69}\text{Ti}_{0.21}\text{Si}_{0.10}$  at room temperature are 4.26 and 4.53 wt.%, respectively. These are somewhat lower compared to the Al-containing alloys because Si is slightly heavier. As the results are similar to the Al addition, the degree of destabilization of the MgTi alloy does not seem to be influenced significantly by the chemistry of the dopant. Furthermore, it shows that the Miedema model

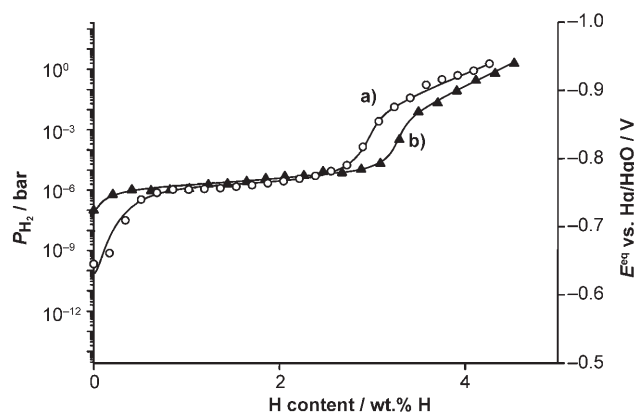


Figure 6. The isothermal curves of 200 nm thick; a)  $\text{Mg}_{0.55}\text{Ti}_{0.35}\text{Si}_{0.10}$  and b)  $\text{Mg}_{0.69}\text{Ti}_{0.21}\text{Si}_{0.10}$  films capped with 10 nm Pd.

can, as a first-order approximation, be used to screen for elements that destabilize a known metal hydrogen system.

## Conclusion

$\text{Mg}_y\text{Ti}_{(1-y)}$  alloys are characterized by isothermal curves with plateau pressures of  $\approx 10^{-6}$  bar at room temperature. Increasing the plateau pressure of a metal-hydrogen system can be accomplished by the destabilization of the metal hydride. The Miedema model was used to screen elements that stabilize the metallic Mg–Ti system and, consequently, destabilize the metal-hydrogen systems. Al and Si were selected to enforce this effect with the additional advantage that these elements are lightweight to maintain the high gravimetric capacity found for  $\text{Mg}_y\text{Ti}_{(1-y)}$  alloys.

Using the galvanostatic intermittent titration technique, pressure-composition isotherms of several  $\text{Mg}_y\text{Ti}_z\text{Al}_{(1-y-z)}$  and  $\text{Mg}_y\text{Ti}_z\text{Si}_{(1-y-z)}$  alloys were determined. The results clearly show that, in line with the results using the Miedema model, the plateau pressure is increased, while maintaining a high gravimetric storage capacity of approximately 6 wt.%. The partial hydrogen pressures of part of the isotherms of the new ternary systems are situated at higher pressures at room temperature. This enables hydrogen storage and release at low temperatures, which is required for many hydrogen-driven devices. The isothermal curves of Mg–Ti–Al and Mg–Ti–Si closely resemble each other and imply that the degree of destabilization does not strongly depend on the chemical properties of the dopants. Hence, in line with Van Mal's rule of reversed stability, destabilization of the MH seems to depend on the thermodynamics of the dopant with the host lattice.

Finally, the possibility to increase the partial hydrogen pressure, while maintaining a high gravimetric capacity creates promising opportunities in the field of hydrogen storage, which are vital to ensure the feasibility of a future hydrogen economy.

## Experimental Section

Thin films of  $\text{Mg}_y\text{Ti}_z\text{Al}_{(1-y-z)}$  and  $\text{Mg}_y\text{Ti}_z\text{Si}_{(1-y-z)}$  were prepared by means of high vacuum deposition (base pressure  $10^{-7}$  mbar). The films, with a nominal thickness of 200 nm, were deposited on quartz substrates (20 mm diameter), which were thoroughly cleaned beforehand. Cap layers of 10 nm Pd were deposited on top of the  $\text{Mg}_y\text{Ti}_z\text{X}_{(1-y-z)}$  (X = Al, Si) layers in order to protect the films against oxidation and to catalyze hydrogen absorption and desorption. The composition and thickness of the as-prepared thin films was checked by means of Rutherford backscattering spectrometry (RBS).

Electrochemical measurements were performed using a three-electrode cell, thermostated at 298 K by means of a water jacket surrounding the cell, filled with 6 M KOH electrolyte in which the thin film acted as working electrode (active surface area of  $3 \text{ cm}^2$ ). The thin films were contacted with a silver wire, which was attached using a conductive adhesive. A chemically inert isolating lacquer was applied to the contacts and the edges of the substrate, shielding them from the electrolyte.

The potential of the working electrode (i.e. metal hydride electrode) was measured with respect to a lead-free Hg/HgO reference electrode (Koslow Scientific Company, USA) filled with a 6 M KOH solution.<sup>[36]</sup> This reference electrode was placed close to the working electrode in order to minimize the Ohmic drop caused by the electrolyte.

The counter electrode, a palladium rod, was placed in a separate compartment in the cell and care was taken that the total area in contact with the electrolyte was sufficiently large. The counter electrode was pre-charged with hydrogen to form  $\text{PdH}_x$ . The total amount of charge required to extract all the hydrogen from this rod far exceeded the charge needed to fully hydrogenate the thin film working electrode. This ensured that during the electrochemical experiments no oxygen was produced at the palladium counter electrode, which is essential, as it is known that  $\text{O}_2$  seriously affects both the electrochemical potential and the hydrogen content of the metal hydride electrode.<sup>[37]</sup> Before commencing with the (de)hydrogenation experiments the strong alkaline solution was de-aerated by purging through the electrolyte with purified Ar for 1 hour. Hereafter, purified Ar was led over the electrolyte, in order not to interfere with the electrochemical potential measurements of the metal hydride electrode. All electrochemical measurements were conducted with an Autolab PGSTAT30 (Ecochemie B.V., The Netherlands).

## Acknowledgements

The authors would like to thank T. Dao for the RBS analyses and D. Danilov for his help with the graphical visualization of our results. Furthermore, financial support from the NWO ACTS Sustainable Hydrogen Program is gratefully acknowledged.

- [1] F. E. Pinkerton, B. G. Wicke, *Ind. Phys.* **2004**, *10*, 20–23.
- [2] W. Doenitz, R. Schmidberger, E. Steinheil, R. Streicher, *Int. J. Hydrogen Energy* **1998**, *23*, 55–63.
- [3] H. Gaffron, J. J. Rubin, *J. Gen. Physiol.* **1942**, *26*, 219–240.
- [4] U. S. Department of Energy, Multi-Year Research, Development and Demonstration, Plan: Planned program activities for 2003–2010, <http://www.eere.energy.gov/hydrogenandfuelcells/mypp/> (May 2007).
- [5] K. H. J. Buschow, P. C. P. Bouten, A. R. Miedema, *Rep. Prog. Phys.* **1982**, *45*, 937–1039.
- [6] J. J. Reilly, R. H. Wiswall, Jr., *Inorg. Chem.* **1968**, *7*, 2254–2256.
- [7] J. F. Stampfer, Jr., C. E. Holley, Jr., J. F. Suttle, *J. Am. Chem. Soc.* **1960**, *82*, 3504–3508.
- [8] R. C. Bowman, B. Fultz, *MRS Bull.* **2002**, *27*, 688–693.
- [9] R. A. H. Niessen, P. H. L. Notten, *Electrochem. Solid-State Lett.* **2005**, *8*, A534–A538.
- [10] P. Vermeulen, R. A. H. Niessen, P. H. L. Notten, *Electrochem. Commun.* **2006**, *8*, 27–32.

- [11] P. Vermeulen, R. A. H. Niessen, D. M. Borsa, B. Dam, R. Griessen, P. H. L. Notten, *Electrochem. Solid-State Lett.* **2006**, *9*, A520–A523.
- [12] D. M. Borsa, A. Baldi, M. Pasturel, P. Vermeulen, P. H. L. Notten, B. Dam, R. Griessen, *Appl. Phys. Lett.* **2006**, *88*, 241910 (1–3).
- [13] A. R. Miedema, P. F. de Châtel, F. R. de Boer, *Physica B + C* **1980**, *100*, 1–28.
- [14] A. R. Miedema, *J. Less-Common Met.* **1973**, *32*, 117–136.
- [15] F. R. de Boer, R. Boom, W. C. M. Mattens, A. R. Miedema, A. K. Niessen in *Cohesion in Metals*, North-Holland, Amsterdam, **1988**.
- [16] H. H. van Mal, K. H. J. Buschow, A. R. Miedema, *J. Less-Common Met.* **1974**, *35*, 65–76.
- [17] K. H. J. Buschow, P. C. P. Bouten, A. R. Miedema, *Rep. Prog. Phys.* **1982**, *45*, 937–1039.
- [18] R. Griessen, T. Riesterer in *Topics in Applied Physics Hydrogen in Intermetallic Compounds*, Vol 63 (Ed. L. Schlapbach), Springer, Berlin, **1988**, 219–284.
- [19] P. Villars in *Pearson's Handbook Desk Edition*, Vol 2, ASM International, Ohio, **1997**, 2336.
- [20] W. P. Kalisvaart, H. J. Wondergem, F. Bakker, P. H. L. Notten, *J. Mater. Res.* **2007**, *22*, 1640–1649.
- [21] P. H. L. Notten, *NATO ASI Ser. E* **1995**, *281*, 151–195.
- [22] J. J. G. Willems, *Philips J. Res. Suppl.* **1984**, *39*, 1–94.
- [23] A. Biris, D. Lupu, R. V. Bucur, E. Indrea, G. Borodi, M. Bogdan, *Int. J. Hydrogen Energy* **1982**, *7*, 89–94.
- [24] F. A. Kuijpers, *J. Less-Common Met.* **1972**, *27*, 27–34.
- [25] J. J. Reilly, R. H. Wiswall, Jr., *Inorg. Chem.* **1974**, *13*, 218–222.
- [26] M. Yamaguchi, T. Katamune, T. Ohta, *J. Appl. Phys.* **1982**, *53*, 2788–2792.
- [27] M. H. Mintz, Z. Gavra, G. Kimmel, *J. Less-Common Met.* **1980**, *74*, 263–270.
- [28] A. Zaluska, L. Zaluski, J. O. Strom-Olsen, *Appl. Phys. A* **2001**, *72*, 157–165.
- [29] S. Bouaricha, J. P. Dodelet, D. Guay, J. Huot, S. Boily, R. Schulz, *J. Alloys Compd.* **2000**, *297*, 282–293.
- [30] H. Takamura, T. Miyashita, A. Kamegawa, M. Okada, *J. Alloys Compd.* **2003**, *356–357*, 804–808.
- [31] L. Pranevicius, D. Milcius, L. L. Pranevicius, G. Thomas, *J. Alloys Compd.* **2004**, *373*, 9–15.
- [32] A. Andreasen, M. B. Sørensen, R. Burkarl, B. Møller, A. M. Molenbroek, A. S. Pedersen, J. W. Andreasen, M. M. Nielsen, T. R. Jensen, *J. Alloys Compd.* **2005**, *404–406*, 323–326.
- [33] R. Gremaud, A. Borgschulte, C. Chacon, J. L. M. van Mechelen, H. Schreuders, A. Züttel, B. Hjörvarsson, B. Dam, R. Griessen, *Appl. Phys. A* **2006**, *84*, 77–85.
- [34] M. Slaman, B. Dam, M. Pasturel, D. M. Borsa, H. Schreuders, J. H. Rector and R. Griessen, *Sens. Actuators B* **2007**, *123*, 538–545.
- [35] D. Lupu, A. Biris, R. V. Bucur, E. Indrea, M. Bogdan, *Met.-Hydrogen Syst., Proc. Miami Int. Symp., Meeting Date 1981*, **1982**, 437.
- [36] R. A. H. Niessen, P. H. L. Notten, *J. Electrochem. Soc.* **2005**, *152*, A2051–A2057.
- [37] R. A. H. Niessen, P. H. L. Notten, *Electrochim. Acta* **2005**, *50*, 2959–2965.

Received: May 16, 2007  
Published online: September 18, 2007